Selected for a Viewpoint in *Physics*
PHYSICAL REVIEW C **84**, 054308 (2011)

Candidate for the 2^+ excited Hoyle state at $E_x \sim 10$ MeV in ^{12}C

M. Itoh,[1] H. Akimune,[2] M. Fujiwara,[3] U. Garg,[4] N. Hashimoto,[3] T. Kawabata,[5] K. Kawase,[3] S. Kishi,[5] T. Murakami,[5] K. Nakanishi,[3] Y. Nakatsugawa,[5] B. K. Nayak,[4] S. Okumura,[3] H. Sakaguchi,[3] H. Takeda,[6] S. Terashima,[5] M. Uchida,[7] Y. Yasuda,[3] M. Yosoi,[3] and J. Zenihiro[3]

[1]*Cyclotron and Radioisotope Center (CYRIC), Tohoku University, Sendai 980-8578, Japan*
[2]*Department of Physics, Konan University, Kobe 658-8501, Japan*
[3]*Research Center for Nuclear Physics (RCNP), Osaka University, Ibaraki, Osaka 567-0047, Japan*
[4]*Physics Department, University of Notre Dame, Notre Dame, Indiana 46556, USA*
[5]*Department of Physics, Kyoto University, Kyoto 606-8502, Japan*
[6]*RIKEN Nishina Center for Accelerator-Based Science, Wako, Saitama 351-0198, Japan*
[7]*Department of Physics, Tokyo Institute of Technology, Tokyo 152-8551, Japan*

(Received 31 May 2011; published 14 November 2011)

Inelastic scattering from ^{12}C has been measured at extremely forward angles including 0° using 386 MeV α particles to study the α-cluster states around $E_x \sim 10$ MeV, especially the 2^+ state predicted by the α-cluster model. We have analyzed (α,α') cross-section data using both peak-fitting and multipole decomposition techniques. A 2^+ state at $E_x = 9.84 \pm 0.06$ MeV with a width of 1.01 ± 0.15 MeV is found to be submerged in the broad 0^+ state at $E_x = 9.93 \pm 0.03$ MeV with a width of 2.71 ± 0.08 MeV. This 2^+ state may be interpreted as the 2^+ excitation of the Hoyle state and the α-condensate state.

DOI: 10.1103/PhysRevC.84.054308 PACS number(s): 21.10.Re, 25.55.Ci, 25.70.Ef, 27.20.+n

I. INTRODUCTION

The ^{12}C nucleus is among the most well-investigated nuclei in the nuclear chart. However, many unanswered questions concerning its nuclear structure still remain. Among them, a persistent question concerns the multipolarity of the broad level at $E_x \sim 10.3$ MeV. In Ref. [1], this state has been tentatively assigned to 0^+. According to the 3α resonating group method (RGM) calculation by Kamimura [2] and Uegaki *et al*. [3], there should be a 2^+ state around $E_x \sim 10$ MeV as the 2^+ member of a β band beginning with the 7.654 MeV 0_2^+ level in ^{12}C, since the coupling strength for the $2_2^+ \rightarrow 0_2^+$ transition is predicted to be 25 times larger than that for the $2_1^+ \rightarrow 0_1^+$ transition. These states have been predicted to be molecule-like states consisting of three α particles.

Tohsaki *et al*. suggested the 0_2^+ state can be a Bose-Einstein condensation-like state, in which all constituent α-clusters condense into the lowest S-wave orbit [4,5]. If a 2^+ state indeed exists in the 10 MeV region, it might be an excited state of the Hoyle state and have a structure similar to the 0_2^+ state in the α-condensate model, in which one of the α clusters occupies a D-wave orbit [6–8]. Although these two pictures are very different, both calculations predicted the existence of a 2^+ state around 10 MeV, which was strongly coupled to the 7.654 MeV 0_2^+ state. Furthermore, there should be a 0_3^+ state in the 10 MeV region, which can be considered as the vibrational mode along the broad energy surface for the 0_2^+ state according to the complex scaling method (CSM) calculation [9], or as the linear-like 3α structure in the antisymmetrized molecular dynamics (AMD) calculation [10].

In addition to the interest in its structure, the 0_2^+ state is very important from the viewpoint of nuclear astrophysics. Hoyle pointed out that the 0_2^+ state is a doorway state, which governs nuclear synthesis heavier than ^{12}C [11]. This state is referred to as the Hoyle state. If an excited state exists closely coupled to the Hoyle state, the elemental abundance of nuclear matter in the universe may be affected. The Nuclear Astrophysics Compilation of Reaction Rates (NACRE) [12], which is widely used in astrophysical calculations, assumes the existence of the 2_2^+ state at $E_x = 9.1$ MeV. However, the exact location of the 2_2^+ state is experimentally unknown, leading to a large uncertainty in the reaction rate of $3\alpha \rightarrow {}^{12}$C.

In terms of experiments, Jacquot *et al*. observed the ^{12}C$(\alpha,\alpha')^{12}$C$^*[3\alpha]$ reaction by using 90 MeV α particles [13]. They claimed the 10.3 MeV state in ^{12}C was a 2^+ state by analyzing the momentum correlation between three α particles emitted therefrom. Motivated by the theoretical prediction in Ref. [2], Brandenburg *et al*. attempted to identify the spin and parity of the broad bump at $E_x \sim 10$ MeV [14]. However, this bump was dominated by the 0^+ component, and no significant 2^+ component was identified. John *et al*. measured inelastic α scattering from ^{12}C at $E_\alpha = 240$ MeV [15]. They analyzed energy spectra by multipole decomposition analysis (MDA) and obtained isoscalar $E0$–$E4$ strengths up to $E_x = 45$ MeV. They reported a 2^+ component located at $E_x = 11.46$ MeV, which is slightly higher than the predicted excitation energy. In 2003, Itoh *et al*. reported the existence of the 2_2^+ state under the broad 0_3^+ bump at $E_x \sim 10$ MeV [16]. After this report, many experimentalists were eager to find out the 2_2^+ state in this excitation-energy region. Recently, Freer *et al*. measured inelastic proton scattering off ^{12}C at 66 and 200 MeV [17]. In their analysis, they included an additional 2^+ state with the width of 600 keV at $E_x = 9.6$ MeV to explain the energy spectrum at 16° where the cross section for the 0^+ state is small in the angular distribution. Muñoz-Britton *et al*. measured the angular correlation for the 3α decay in the ^{12}C(^{12}C,^{12}C[3α]) reaction [18]. However, no conclusive result for the 2_2^+ state was obtained.

Fynbo *et al.* examined the spin and parity of the excited states in ^{12}C fed by the β decay of ^{12}B and ^{12}N [19]. They showed that the energy spectra around $E_x \sim 10$ MeV is well reproduced by taking the interference between the 0_2^+ state at $E_x = 7.654$ MeV and the 0_3^+ state at $E_x = 11.2$ MeV into account in the R-matrix analysis, and no 2^+ state is necessary around $E_x \sim 10$ MeV to explain their data. Recently, the same group obtained data with improved statistics and revised their R-matrix analysis [20]. They showed the existence of the broad 11.2 MeV 0^+ and 11.1 MeV 2^+ states.

Very recently, M. Gai *et al.* performed the ^{12}C(γ,3α) experiment at the High Intensity Gamma-Ray Source (HIGS) facility at Duke University [21]. They measured three decay α's with an optical readout time projection chamber (O-TPC) and observed a pure $E2$ angular distribution most likely arising from a 2^+ state below 10 MeV. Although their preliminary result showed the existence of a 2^+ state, to date they have not reported its energy and width.

The experimental situation concerning the 2_2^+ state in ^{12}C is, thus, still controversial, and it is highly desirable to obtain conclusive evidence for the 2_2^+ state. In this paper, we report on two kinds of alternate analyses on inelastic α-scattering data we had measured precisely for ^{12}C nucleus at $E_\alpha = 386$ MeV. One of them is peak-fitting analysis to ensure the existence of the 2^+ state and to obtain its strength. The other is MDA with a more realistic density predicted by the α-cluster model than the previously adopted one in order to extract the reliable strength distributions of the 2^+ state and the broad 0^+ state. We find clear evidence for the second 2^+ state at $E_x = 9.84 \pm 0.06$ MeV.

II. EXPERIMENT

The experiment was performed at the ring cyclotron facility of the Research Center for Nuclear Physics (RCNP), Osaka University, using the Grand Raiden spectrometer [22]. Details of the experimental setup and procedure are described in Ref. [23], and only a brief outline is provided below.

Inelastic scattering of 386 MeV α particles off ^{12}C has been measured at forward angles between $\theta = 0^\circ$ and 15°. "Background-free" inelastic-scattering spectra were obtained at all angles, including 0°. A self-supporting natural carbon foil with a thickness of 2.84 mg/cm^2 was used. The target foil contained oxygen and hydrogen (about 3%) from the glue that was used in the preparation of the target. The contribution from the oxygen contaminant was estimated using ^{28}Si and SiO$_2$ data and subtracted from the energy spectra. The data at crossover angles between inelastic scattering from ^{12}C and elastic scattering from hydrogen were not included in the analysis.

In the normal magnetic field setting of the Grand Raiden, particles scattered from the target are focused vertically and horizontally at the focal plane. On the other hand, instrumental background events due to rescattering of α particles on the wall and pole surfaces of the spectrometer are not focused in the vertical direction. Thus, we obtained background-free spectra by subtracting events at the off-median plane from those at the median plane. The energy spectra were measured in the range of $7 \leqslant E_x \leqslant 30$ MeV at 0° and $3 \leqslant E_x \leqslant 30$ MeV at 2°–15°.

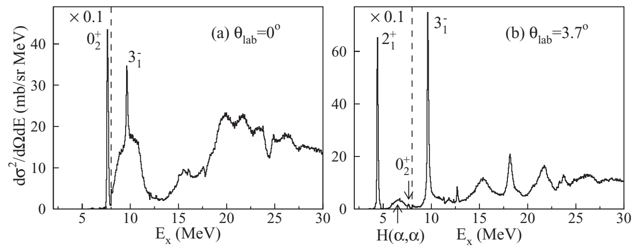

FIG. 1. Energy spectra for the ^{12}C(α,α') reaction at scattering angles (a) $\theta_{\rm lab} = 0^\circ$ and (b) $\theta_{\rm lab} = 3.7^\circ$. The momentum acceptances of the spectrometer were in the range of $3 \leqslant E_x \leqslant 30$ MeV at 2.0°–15° and of $7 \leqslant E_x \leqslant 30$ MeV at 0°, respectively.

Figure 1 shows typical energy spectra for the ^{12}C(α,α') reaction at $\theta_{\rm lab} = 0^\circ$ and 3.7°, where differential cross sections are at maximum for angular momentum transfer $L = 0$ and 2, respectively. At 0°, the most prominent peak is the 0_2^+ state at $E_x = 7.654$ MeV. The broad bump at $E_x \sim 10$ MeV is also observed underneath the sharp 3_1^- state at $E_x = 9.641$ MeV. Since the cross section for the $L = 0$ transition becomes quite small at 3.7°, the 0_2^+ peak is almost invisible on the tail of the hydrogen contaminant bump. The broad bump around $E_x \sim$ 10 MeV also becomes small because this bump is dominated by the 0^+ component. However, a sizable strength remains around $E_x \sim 10$ MeV. It suggests the broad bump contains higher multipole components with $L \neq 0$. To investigate the states at $E_x \sim 10$ MeV by means of MDA with a small energy-bin size, special care was exercised to keep the energy resolution of the beam stable. The energy resolution was about 200 keV through all runs.

Elastic scattering from ^{12}C was also measured at $\theta_{\rm c.m.} = 4^\circ$–$35^\circ$ to determine the phenomenological N-α interaction parameters with the same incident energy. The thickness of the carbon-graphite target for the measurement of elastic scattering was 30 mg/cm^2.

III. DISTORTED-WAVE BORN APPROXIMATION CALCULATION

Distorted-wave Born approximation (DWBA) calculations were carried out in the framework of the single-folding model with a density-dependent effective N-α interaction [24] to obtain the angular distributions for various multipole components. The density-dependent effective N-α interaction was given as

$$V(|\mathbf{r}-\mathbf{r}'|,\rho_0(r')) = -V[1+\beta_V\rho_0(r')^{2/3}]\exp(-|\mathbf{r}-\mathbf{r}'|^2/\alpha_V) - iW[1+\beta_W\rho_0(r')^{2/3}]\exp(-|\mathbf{r}-\mathbf{r}'|^2/\alpha_W). \tag{1}$$

The parameters, $V = 36.73$ MeV, $W = 25.9$ MeV, and $\alpha_{V,W} = 3.7$ fm^2 were obtained by fitting the measured elastic scattering angular distribution, as shown in Fig. 2. The density-dependent coefficients, $\beta_{V,W} = -1.9$ fm^2, were taken from Ref. [25]. The ground-state density $\rho_0(r)$ was obtained by unfolding from the charge density measured by electron scattering [26] and the nucleon form factor [27]. The calculations were performed by using the code ECIS95 [28] with external form factors obtained

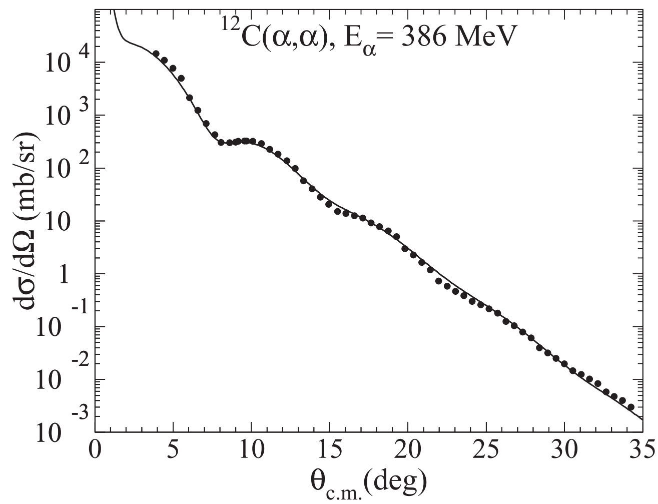

FIG. 2. Angular distribution of elastic scattering from ^{12}C at $E_\alpha = 386$ MeV. The solid line shows the result of the DWBA calculation using the single-folding model with the effective N-α interaction.

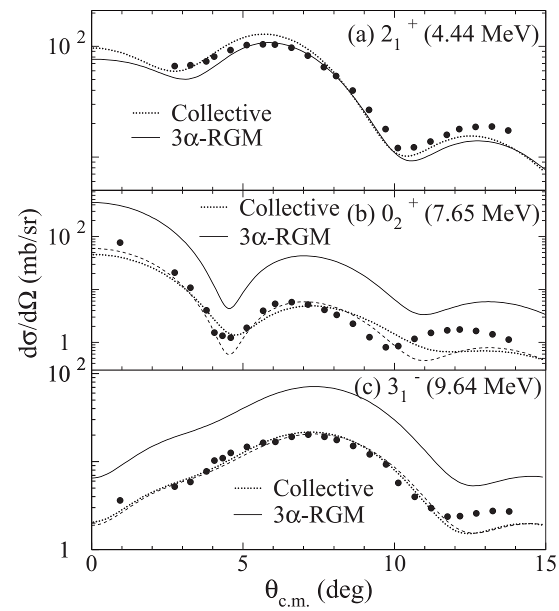

FIG. 3. Angular distributions of inelastic α scattering to (a) the 4.44 MeV 2_1^+ state, (b) the 7.65 MeV 0_2^+ state, and (c) the 9.64 MeV 3_1^- state at $E_\alpha = 386$ MeV. The solid and dotted lines show the result of the DWBA calculation with the 3α RGM and collective models, respectively. The dashed lines show the 3α RGM calculations normalized to the experimental data.

by three models: the collective model [25,29]; the 3α RGM model [2]; and the α-condensate model [30]. Figure 3 shows the angular distributions of (a) the 4.44 MeV 2_1^+, (b) the 7.65 MeV 0_2^+, and (c) the 9.64 MeV 3_1^- states. Yields of the 0_2^+ and the 3_1^- states were extracted from the peak-fitting analysis explained in the next section. Absolute values of the angular distributions using collective transition densities are fitted to the experimental data. Although all of the calculations reproduced the experimental data up to 10° quite well, the fits corresponding to the 3α RGM model were better than those from the collective model.

The reduced electric transition rates, $B(EL)$, are obtained from the 2^L-pole transition moment as

$$B(EL) = \left|\frac{Z}{A}\int \rho_L^{\rm tr}(r) r^{L+2} dr\right|^2 e^2 \quad (L \geqslant 2), \qquad (2)$$

where A, Z, and $\rho_L^{\rm tr}(r)$ are the mass number, the atomic number, and the transition density for the angular momentum transfer, L, respectively. The $B(E2)$ value of the 2_1^+ state obtained by the collective transition density is $37 \pm 1\ e^2\ \mathrm{fm}^4$. The $B(E3)$ value of the 3_1^- state is $251 \pm 10\ e^2\ \mathrm{fm}^6$. These values are in good agreement with those obtained by inelastic α scattering at 240 MeV [15]. In the case of the 3α RGM calculation, normalization is needed for the 0_2^+ and the 3_1^- states, respectively, as shown by the dashed lines in Fig. 3. The calculation reproduces angular distributions of the 0_2^+ and the 3_1^- states up to 10°. The calculation for the 2_1^+ state reproduces the experimental data quantitatively.

IV. PEAK-FITTING ANALYSIS

In order to confirm the existence of the 2^+ component, we performed a peak-fitting analysis of the excitation-energy spectra. In the $E_x \sim 10$ MeV region, there are several known states. Each of the 7.65 MeV 0_2^+ and the 9.64 MeV 3_1^- states was fitted with two Gaussian functions to obtain better results for the fits. Since their intrinsic widths were smaller than the energy resolution of this experiment, their peak shapes reflect the structure of the beam. Broad peaks, such as the 10.3 MeV 0_3^+ and the 10.84 MeV 1_1^-, were fitted with a single Gaussian function. An additional peak around 8.5 MeV was needed to fit energy spectra at $\theta_{\rm lab} = 0^\circ$, 1.9°, and 2.3°, as shown in Fig. 4. We have established that this additional peak does not come from the oxygen contaminant. The contribution from the oxygen contaminant has already been subtracted, as described in Sec. II. Furthermore, the unnatural-parity 2^- state at $E_x = 8.87$ MeV in ^{16}O would be excited only very weakly, at best, by the spin-0 (α,α') reaction. Therefore, the yield of this additional peak of 8.5 MeV was added to that of the broad bump. From the broad-bump spectrum, shown in Fig. 4, we subtracted the yields of the well-known states—7.65 MeV 0_2^+, 9.64 MeV 3_1^-, and 10.84 MeV 1_1^-—using peak-fitting analysis and, thus, obtained the yield of the broad bump itself.

Figure 5 shows the angular distribution of the broad bump, which is fitted with the $L = 0$ and $L = 2$ angular distributions. The absolute differential cross sections for these transitions were arranged to explain the experimental angular distribution as follows:

$$\sigma^{\rm exp}(\theta) = \sum_{L=0,2} a_L\, \sigma_L^{\rm calc}(\theta). \qquad (3)$$

The $L = 0$ and $L = 2$ angular distributions were calculated by using the transition density of the collective and α-condensed model [30], respectively. Reduced χ^2 of the fit to the experimental angular distribution is 75. If we fit this experimental angular distribution without the $L = 0$ or $L = 2$ transitions, the reduced χ^2 are 819 and 1097, respectively. If we use the $L = 2$ angular distribution calculated by the

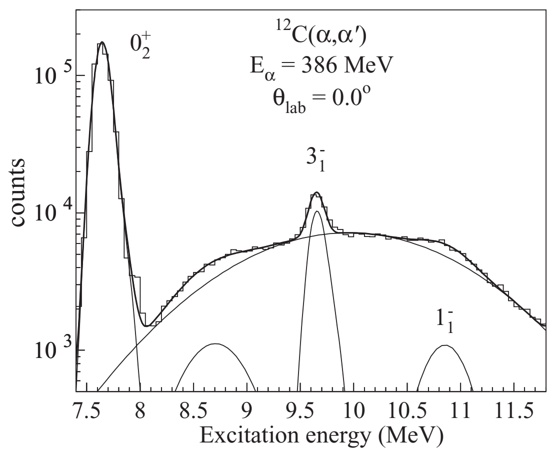

FIG. 4. Excitation-energy spectrum for ^{12}C fitted to the 7.65 MeV 0_2^+, 9.64 MeV 3_1^-, 10.84 MeV 1_1^-, and the 10 MeV broad bump at 0°. The thick line shows the fitting result. The thin solid lines show the individual peaks. The additional peak around 8.5 MeV was needed to fit at 0°, 1.9°, and 2.3°.

collective model, the reduced χ^2 becomes worse. In order to estimate contributions from other multipole components, we also fitted the angular distribution with the $L = 0$, 1, 2, 3 transitions. There was no $L = 3$ contribution. However, a small contribution for the $L = 1$ transition might remain in the broad bump. This could be caused by a failure to fit the broad bump with a single Gaussian function. However, since it was less than 6% at the maximum angle for the $L = 1$ contribution, the existence of the 2^+ state together with the broad 0^+ state may be inferred. The $B(E2)$ value obtained from the transition density of the α-condensed model is 1.83 ± 0.09 e^2 fm^4. The $E0$ strength of the 0_2^+ state obtained by inelastic α scattering was very sensitive to the interaction parameters and the transition densities and was significantly smaller than that obtained by the (e, e') data [31].

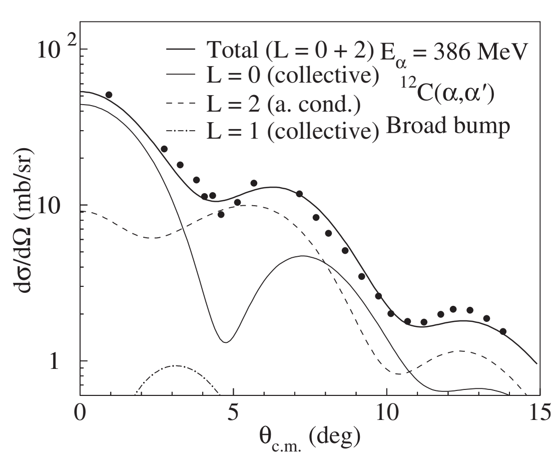

FIG. 5. Angular distribution of inelastic α scattering to the broad bump around 10 MeV. The thin solid and dashed lines show the angular distributions calculated using the collective ($L = 0$) and the α-condensed model [30] ($L = 2$) transition densities, respectively. The thick solid line shows the sum of the $L = 0$ and 2 angular distributions. The dot-dashed line shows the possible $L = 1$ component.

We, therefore, show just the ratio of the $E0$ strength between $B(E0;0_1 \rightarrow 0_3)$ and $B(E0;0_1 \rightarrow 0_2)$ obtained from the same model. The $B(E0)$ value is obtained as follows:

$$B(E0) = \left| \frac{Z}{A} \int \rho_0^{\mathrm{tr}}(r) r^4 dr \right|^2 e^2. \tag{4}$$

The $B(E0;0_1 \rightarrow 0_3)/B(E0;0_1 \rightarrow 0_2)$ obtained by the collective and the 3α RGM models are 1.0 and 0.84, respectively.

V. MULTIPOLE DECOMPOSITION ANALYSIS

In order to find the strength distributions for the 0_3^+ and the 2_2^+ states, we performed MDA with the small energy-bin size. The angular distributions of the double-differential cross sections were obtained by dividing the energy spectrum into 0.25-MeV bins and sorting in terms of scattering angles. Since the DWBA calculation reproduces well the experimental angular distributions for the 2_1^+, the 0_2^+, and the 3_1^- states up to 10° as shown in the previous section, we used the experimental data up to 10° in the MDA. Inelastic α scattering has a selectivity for the isoscalar natural-parity transition, and its angular distributions are characterized by the transferred angular momentum L. In MDA, the experimentally obtained cross sections are expressed as the sum of the contributions from the various multipole components as

$$\sigma^{\exp}(\theta, E_x) = \sum_L a_L(E_x)\, \sigma_L^{\mathrm{calc}}(\theta, E_x), \tag{5}$$

where E_x, θ are the excitation energy and the scattering angle, respectively, and $\sigma_L^{\mathrm{calc}}(\theta, E_x)$ is the DWBA cross section for the transferred angular momentum L. Multipole components up to $L = 5$ were taken into account in the fit, since the first maximum of the angular distribution for the $L = 5$ transfer appears at 10°. To obtain a better fit with the MDA, the angular distributions for $L = 0$ and 3 were calculated by the 3α RGM model, and that for $L = 2$ was calculated by the α-condensate model [30]. Those for other multipole transitions were calculated by the collective model [25,29]. In the MDA, the shape of the strength distribution is roughly determined by L. However, since the differences between the transition densities for the collective and cluster models are large, the fits are better for the chosen models.

Figure 6 shows the angular distribution for each energy bin of 0.25 MeV. The solid lines show the fits to the experimental data. They reproduce the angular distribution of each energy bin very well. Figure 7 shows the energy spectra and the results of the MDA at (a), (c) $\theta_{\mathrm{lab}} = 0°$, and (b), (d) $\theta_{\mathrm{lab}} = 3.7°$, respectively. The broad bump at 0° is dominated by the $L = 0$ component. On the other hand, that at $\theta_{\mathrm{lab}} = 3.7°$ is dominated by the $L = 2$ component. Figure 8 shows the isoscalar-strength distributions for the $L = 0$, 1, 2, and 3 transitions. The isoscalar-strength distributions were extracted from the following equations:

$$S_L(E_x) = a_L(E_x) \left| \int \rho_L^{\mathrm{tr}}(r, E_x) r^{L+4} dr \right|^2 (L = 0, 1), \tag{6}$$

$$S_L(E_x) = a_L(E_x) \left| \int \rho_L^{\mathrm{tr}}(r, E_x) r^{L+2} dr \right|^2 (L \geqslant 2). \tag{7}$$

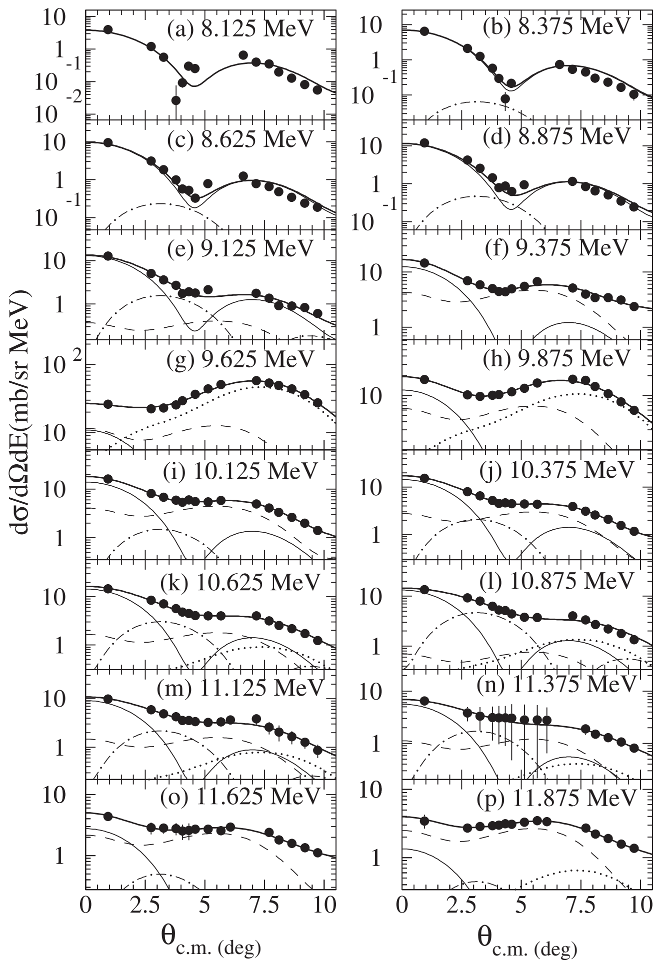

FIG. 6. Angular distributions of the double-differential cross section at E_x = 8–12 MeV for various excitation-energy bins in ^{12}C. The thick solid lines show the fits to the data from multipole decomposition. In each panel, the contributions from $L = 0$ (thin solid), $L = 1$ (dot-dashed), $L = 2$ (dashed) and $L = 3$ (dotted) are also displayed. Contributions from other multipoles are not displayed.

In the calculations with the 3α RGM model and the α-condensate model, we assumed that there were no excitation-energy dependences of the transition densities. The well-known 3_1^- state at $E_x = 9.64$ MeV and the 1_1^- state at $E_x = 10.84$ MeV are clearly seen in Figs. 8(d) and 8(b), respectively. In addition to these, one sees the broad 0^+ strength at $E_x = 9.93 \pm 0.03$ MeV with a width of 2.71 ± 0.08 MeV, and the 2^+ strength at $E_x = 9.84 \pm 0.06$ MeV with a width of 1.01 ± 0.15 MeV, even though the MDA uncertainties in the $L = 0$ and $L = 2$ strengths are large at $E_x = 9.64$ MeV because of the strong 3_1^- state at about the same energy. Following conventional procedures, the positions and widths of these states were obtained by fitting each with a single Gaussian function. The 2^+ state, predicted by several theories [2,3,6,9], has been confirmed. The $B(E2)$ value obtained by integrating the $L = 2$ strength distribution from 9 to 11 MeV and multiplying a factor of $e^2/4$ is $1.6 \pm 0.2\ e^2\ \mathrm{fm}^4$. This value is consistent with the result of the peak-fitting analysis reported earlier in the paper.

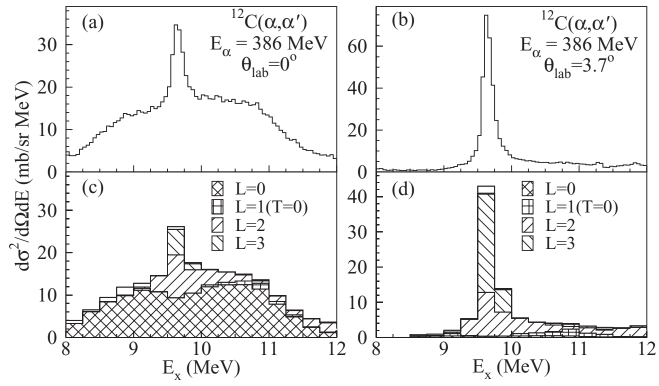

FIG. 7. Excitation-energy spectra from $^{12}\mathrm{C}(\alpha,\alpha')$ at $\theta_{\mathrm{lab}} = 0^\circ$, 3.7°. The hatched regions were constructed from the results of the MDA. The cross-hatched region is $L = 0$, the right-hatched is $L = 2$, the left-hatched is $L = 3$, and the vertical-hatched regions represent contributions from other multipoles.

VI. DISCUSSION

The newly found 2_2^+ state is located at $E_x = 9.84 \pm 0.06$ MeV with a width of 1.01 ± 0.15 MeV, both values close to those predicted by many α-cluster model calculations [2,3,6,9], using 2^+ wave functions strongly coupled to the Hoyle state. This correspondence strongly suggests that the 2_2^+ state has a highly developed 3α structure, and is inferred to be an excited state of the Hoyle state. It is noted that the existence of the 2_2^+ state at 9.6 MeV in ^{12}C has been discussed by Zimmerman *et al.* [32]. This 2_2^+ state at 9.6 MeV would correspond to the 9.84 MeV 2_2^+ state in ^{12}C, which is reported in this paper. The astrophysical NACRE [12]

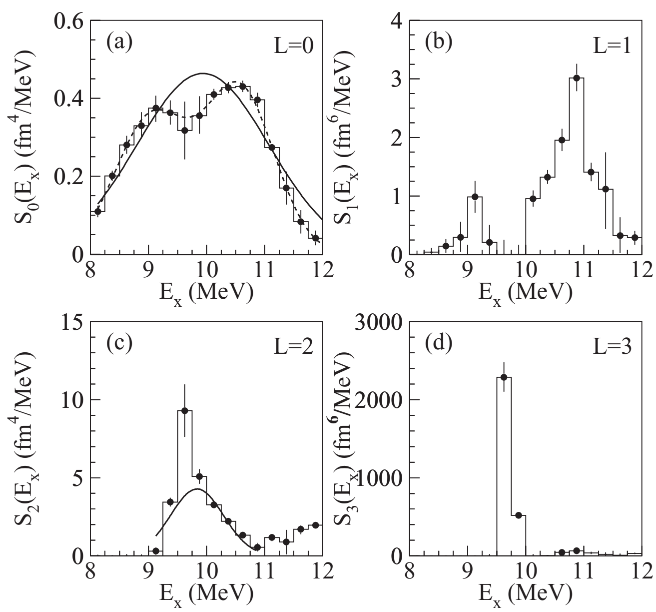

FIG. 8. Isoscalar-strength distributions for (a) $L = 0$, (b) $L = 1$, (c) $L = 2$, and (d) $L = 3$ as obtained in this paper. The vertical axes show the corresponding isoscalar strengths. The solid lines show the conventional fit by a Gaussian function in (a) and (c). The dashed line in (a) shows the fit by two Gaussian functions.

includes the existence of the 2^+ state at $E_x = 9.1$ MeV, which has not been experimentally observed. Fynbo *et al.* [19] had excluded the 9.1 MeV 2^+ contribution according to their β-decay experiment. However, since the strength distribution for the 2_2^+ state obtained in our experiment rises from $E_x \sim 9$ MeV as shown in Fig. 8(c), it is imperative that astrophysical calculations include effects of this broad 2_2^+ state.

The 2^+ state at 11.46 MeV, which was reported in Ref. [15], was not observed in the present experiment. Neither could we discern any peaks corresponding to the 0^+ state at $E_x = 11.2$ MeV or the 2^+ state at $E_x = 11.1$ MeV, reported in Ref. [20]. On the other hand, the broad 0_3^+ state at $E_x = 9.93 \pm 0.03$ MeV with a width of 2.71 ± 0.08 MeV is in good agreement with that measured in inelastic α scattering at $E_\alpha = 240$ MeV [15]. However, the strength distribution has an asymmetric shape, which may be due to two different 0^+ states. As shown in Fig. 8(a), these two states are located at $E_x = 9.04 \pm 0.09$ MeV with a width of 1.45 ± 0.18 MeV and at $E_x = 10.56 \pm 0.06$ MeV with a width of 1.42 ± 0.08 MeV, respectively, and may correspond to the 0_3^+ and 0_4^+ states described in Ref. [9]. Further investigations of the microscopic structure of these states are needed, both experimentally and theoretically.

VII. CONCLUSION

We have measured inelastic scattering of α particles at $E_\alpha = 386$ MeV from ^{12}C. The angular distributions of the differential cross sections from $\theta = 0^\circ$ to 10° and from $E_x = 3$ to 30 MeV were obtained. By using a peak-fitting analysis, the angular distribution for the broad bump around $E_x = 10$ MeV was extracted and analyzed using a DWBA calculation. The strength distribution for the $L = 0, 1, 2, 3$ transitions was extracted by the MDA. As a result, a broad 0_3^+ state at $E_x = 9.93 \pm 0.03$ MeV with a width of 2.71 ± 0.08 MeV and a broad 2_2^+ state at $E_x = 9.84 \pm 0.06$ MeV with a width of 1.01 ± 0.15 MeV were clearly identified. This 2_2^+ state is a good candidate for the excited state of the Hoyle resonance and also the α-particle condensate state.

ACKNOWLEDGMENTS

The authors acknowledge RCNP cyclotron staff for providing a very stable and high-quality beam for the 0° and extremely forward angle measurements. The authors also acknowledge Dr. Y. Funaki for providing the transition density of the 2_2^+ state and for stimulating discussions. Thanks are also due to Profs. H. Horiuchi and A. Tohsaki for their interest and for many discussions concerning this experiment. This work was performed under the RCNP E200 program and supported in part by Grant Aid for Scientific Research No. 19740119 from the Japanese Ministry of Education, Sports, Culture, Science, and Technology and the United States National Science Foundation (Grants No. INT03-42942, PHY07-58100, and PHY-1068192).

[1] F. Ajzenberg-Selove, Nucl. Phys. A **506**, 1 (1990).
[2] M. Kamimura, Nucl. Phys. A **351**, 456 (1981).
[3] E. Uegaki, S. Okabe, Y. Abe, and H. Tanaka, Prog. Theor. Phys. **57**, 1262 (1977).
[4] A. Tohsaki, H. Horiuchi, P. Schuck, and G. Röpke, Phys. Rev. Lett. **87**, 192501 (2001).
[5] H. Horiuchi, in *Clusters in Nuclei,* Lecture Notes in Physics Volume 818, edited by C. Beck (Springer-Verlag, Berlin, 2010), p. 57.
[6] Y. Funaki, A. Tohsaki, H. Horiuchi, P. Schuck, and G. Röpke, Eur. Phys. J. A **24**, 321 (2005).
[7] T. Yamada and P. Schuck, Phys. Rev. C **69**, 024309 (2004).
[8] T. Yamada *et al.*, in *Clusters in Nuclei,* Lecture Notes in Physics, edited by C. Beck, Vol. 2 (Springer-Verlag, Berlin, 2010).
[9] C. Kurokawa and K. Kato, Nucl. Phys. A **792**, 87 (2007).
[10] Y. Kanada-En'yo, Prog. Theor. Phys. **117**, 655 (2007); Y. Kanada-En'yo and M. Kimura, in *Clusters in Nuclei,* Lecture Notes in Physics Volume 818, edited by C. Beck (Springer-Verlag, Berlin, 2010), p. 129.
[11] F. Hoyle, Astrophys. J. Suppl. Ser. **1**, 121 (1954).
[12] C. Angulo *et al.*, Nucl. Phys. A **656**, 3 (1999).
[13] C. Jacquot, Y. Sakamoto, M. Jung, and L. Girardin, Nucl. Phys. A **201**, 247 (1973).
[14] S. Brandenburg, A. Drentje, M. Harakeh, and A. van der Woude, KVI Annual Report, 1985 (unpublished).
[15] B. John, Y. Tokimoto, Y.-W. Lui, H. L. Clark, X. Chen, and D. H. Youngblood, Phys. Rev. C **68**, 014305 (2003).
[16] M. Itoh *et al.*, Nucl. Phys. A **738**, 268 (2004).
[17] M. Freer *et al.*, Phys. Rev. C **80**, 041303(R) (2009).
[18] T. Muñoz-Britton *et al.*, J. Phys. G **37**, 105104 (2010).
[19] H. O. U. Fynbo *et al.*, Nature (London) **433**, 136 (2005).
[20] S. Hyldegaard *et al.*, Phys. Rev. C **81**, 024303 (2010).
[21] M. Gai for the UConn-Yale-Duke-Weizmann-PTB-UCL Collaboration, J. Phys. C **267**, 012046 (2011); for the UConn-Yale-Duke-Weizmann-PTB-UCL Collaboration, Acta Phys. Pol. B **42**, 775 (2011).
[22] M. Fujiwara *et al.*, Nucl. Instrum. Methods Phys. Res., Sect. A **422**, 484 (1999).
[23] M. Itoh *et al.*, Phys. Rev. C **68**, 064602 (2003).
[24] A. Kolomiets, O. Pochivalov, and S. Shlomo, Phys. Rev. C **61**, 034312 (2000).
[25] G. R. Satchler, Nucl. Phys. A **472**, 215 (1987).
[26] H. De Vries *et al.*, At. Data Nucl. Data Tables **36**, 495 (1987).
[27] H. Sakaguchi, Memoirs of the Faculty of Science, Kyoto University, Series of Physics, Astrophysics, Geophysics and Chemistry **36**, Article 4 (1982).
[28] J. Raynal, computer code, ECIS95, NEA0850-14.
[29] M. Harakeh and A. van der Wounde, *Giant Resonances* (Clarendon, Oxford, 2001).
[30] Y. Funaki, A. Tohsaki, H. Horiuchi, P. Schuck, and G. Röpke, Eur. Phys. J. A **28**, 259 (2006).
[31] P. Strehl, Z. Phys. **234**, 416 (1970).
[32] W. R. Zimmerman, N. E. Destefano, M. Freer, M. Gai, and F. D. Smit, Phys. Rev. C **84**, 027304 (2011).